

Sonochemical Preparation and Characterization of Ultrafine Chromium Oxide and Manganese Oxide Powders

N. Arul Dhas, Y. Koltypin, and A. Gedanken^{*,†}

Department of Chemistry, Bar-Ilan University, Ramat-Gan, 52900, Israel

Received July 2, 1997. Revised Manuscript Received October 10, 1997[®]

Ultrafine powders of chromium oxide (Cr₂O₃) and manganese oxide (Mn₂O₃) have been prepared at room temperature by the sonochemical reduction of an aqueous solution containing ammonium dichromate [(NH₄)₂Cr₂O₇] and potassium permanganate (KMnO₄), respectively. The yield of the sonochemical reduction has been enhanced by raising the reaction temperature or by using an aqueous solution of ethanol (0.1 M). The solid oxide residue formed on insonation has been characterized by X-ray diffraction (XRD), infrared spectroscopy (IR), differential scanning calorimetry (DSC), elemental analysis, electron microscopy (TEM, SEM/EDX), powder density, particle size (adsorption and microscopy), and BET surface area measurements. The powders are nanosized (50–200 nm), and the surface area varies from 35 to 48 m²/g. The as-formed X-ray amorphous Mn₂O₃ and Cr₂O₃ powders were converted into crystalline form by heating them at 600 and 900 K, for 4 h, respectively.

1. Introduction

Transition metal oxides have drawn a great deal of attention in recent years, due to their very attractive physical, chemical, and magnetic properties.¹ The increasing interest in the study of simple and mixed transition metal oxides is attributed to a myriad of application in the fields of refractory, ceramic colors, catalysis, energy conversion/storage, optics, magnetics, and electronics. Currently, considerable amount of attention has been focused on the preparation of amorphous nanophase materials, particularly oxides, using wet-chemical or soft-chemical methods; that has advantages over the traditional solid-state methods in terms of processing temperature, purity, size, morphological control, and reactivity.² Various methods are used to prepare chromium oxide (Cr₂O₃) and manganese oxide (Mn₂O₃) powders, including the sol–gel method,^{2a} thermal decomposition,^{2b} γ -ray radiation,^{2c} precipitation,^{2d} and citrate route.^{2e} However, the particle sizes of Cr₂O₃ and Mn₂O₃ powders prepared by these methods are relatively large. Furthermore, thermal treatment is necessary in some methods and this is not favorable for synthesis of nanometer-size Cr₂O₃ and Mn₂O₃ powders with a narrow size distribution.

Recently Suslick and co-workers³ reported the preparation of nanostructured amorphous metals by a novel sonochemical method involving the irradiation of a metal carbonyl in a nonaqueous medium by high-

intensity ultrasound radiation. This method is based on the cavitation phenomenon, viz. the formation, growth, and implosive collapse of bubbles in a liquid medium.⁴ The extremely high temperatures and very high cooling rates (>10⁷ K/s) attained during cavitation have been exploited in this method to dissociate metal carbonyl bonds to form nanostructured amorphous metals. Adopting similar techniques, we have reported^{5,6} the preparation of amorphous Ni and Fe₂O₃ in nonaqueous media without any glass forming additives.

The formation of various colloidal systems such as metal sols, metal oxides, metal sulfides, etc. in an aqueous medium by the application of ultrasound irradiation has been reviewed by Grieser.⁷ It has been recognized that the absorption of ultrasound by water can lead to the formation of H atoms, and OH radicals, and that these species may subsequently initiate a variety of chemical reactions depending on the solutes present in solution.^{7–9} Gutierrez et al.⁸ reported the formation of various different colloidal materials by the reduction of metal ions with H atoms produced ultrasonically in water. They have obtained colloidal MnO₂ by a controlled sonochemical reduction of KMnO₄ under an Ar–hydrogen atmosphere. Grieser and co-workers^{7,9} investigated the dissolution of MnO₂ colloids induced by ultrasound in an aqueous medium. Moser and co-workers¹⁰ have prepared a large number of simple and mixed oxides using the ultrasound irradiation. They

[†] E-mail: gedanken@ashur.cc.biu.ac.il.

[®] Abstract published in *Advance ACS Abstracts*, November 15, 1997.

(1) *Transition Metal Oxides*, Rao, C. N. R., Raveau, B., Eds.; VCH: Weinheim, 1995.

(2) (a) Chatterjee, M.; Siladitya, B.; Ganguli, D. *Mater. Lett.* **1995**, *25*, 261. (b) Gubrynowicz, L.; Stromich, T. *Thermochim. Acta* **1987**, *115*, 137. (c) Yingjie, Z.; Yitai, Q.; Manwei, Z. *Mater. Sci. Eng. B* **1996**, *41*, 294. (d) Sohn, J. R.; Tyu, S. G.; Park, M. Y.; Pae, Y. I. *J. Mater. Sci.* **1993**, *28*, 4651. (e) Sugawara, M.; Ohno, M.; Matsuki, K. *Chem. Lett.* **1991**, 1465.

(3) Suslick, K. S.; Choe, S. B.; Cichowlas, A. A.; Grinstaff, M. W. *Nature* **1991**, *353*, 414.

(4) *Ultrasound: Its Chemical, Physical and Biological Effects*. Suslick, K. S., Ed.; VCH: Weinheim, 1988.

(5) Koltypin, Y.; Katabi, G.; Prozorov, R.; Gedanken, A. *J. Non-Cryst. Solids* **1996**, *201*, 159.

(6) Cao, X.; Koltypin, Y.; Katabi, G.; Prozarov, R.; Gedanken, A. *J. Mater. Res.* **1997**, *12*, 402.

(7) Grieser, F. *Stud. Surf. Sci. Catal.* **1997**, *103*, 57.

(8) Gutierrez, M.; Henglein, A.; Dohrmann, J. *J. Phys. Chem.* **1987**, *91*, 6687.

(9) Sostaric, J. Z.; Mulvaney, P.; Grieser, F. *J. Chem. Soc., Faraday Trans.* **1995**, *91*, 2843.

(10) Moser, W. R. private communication.

claim that the ultrasound-derived amorphous oxide materials are highly pure compared to those obtained by the classical methods. However, the potential of the sonochemical method for the preparation of amorphous transition metal oxides in aqueous media has not been exploited so far. Here we report the preparation of amorphous Cr_2O_3 and Mn_2O_3 by the sonochemical reduction of $(\text{NH}_4)_2\text{Cr}_2\text{O}_7$ and KMnO_4 , respectively, in an aqueous medium at room temperature.

2. Experimental Section

Amorphous powders of Cr_2O_3 and Mn_2O_3 have been obtained by the sonochemical reduction of $(\text{NH}_4)_2\text{Cr}_2\text{O}_7$ and KMnO_4 , respectively, in an aqueous medium at room temperature. Typically, 13 g of $(\text{NH}_4)_2\text{Cr}_2\text{O}_7$ was dissolved in 50 mL of distilled water in a sonication flask (total capacity 55 mL, diameter 26 mm o.d.). The resulting saturated solution was exposed to high-intensity ultrasound radiation for 3 h by employing a direct immersion titanium horn (Vibracell, horn diameter 1.13 cm, power 600 W) operating at 20 kHz, with an intensity of 100 W/cm^2 , under argon at a pressure of approximately 1.5 atm. The titanium horn was inserted to a depth of ~ 1 cm in the solution. The sonication cell was kept immersed in a cold bath containing ice during the entire sonication. The temperature of the reaction solution rose to 290 ± 5 K during sonication. The resulting solid product was washed thoroughly with hot water and ethanol and dried in vacuum (yield ~ 3.2 g, 40%).

Amorphous Mn_2O_3 powder was prepared by the ultrasound irradiation of a saturated solution of KMnO_4 (10 g in 50 mL of water) under similar conditions to those described above. The resulting brownish black solid residue was washed thoroughly with hot water, dilute HCl, and ethanol and dried in a vacuum (yield ~ 2.2 g, 45%). The yield of both products can be enhanced (yield 60–70%) by using 0.1 M ethanol or by increasing the reaction temperature to 340 ± 5 K.

The X-ray diffraction patterns of the produced solids were obtained with a Rigaku X-ray diffractometer (Model-2028, Cu K α). Domain size was calculated from the X-ray line broadening using Debye–Scherrer equation.¹¹ Infrared (IR) spectra were recorded by employing a Nicolet (impact 410) FT-IR spectrometer using a KBr pellet. Differential scanning calorimetry (DSC) of dried products was carried out on a Mettler DSC-30 instrument with a heating rate of 10 K/min. Classical elemental analyses and the ICP technique were used to determine the composition of the products. Elemental composition was also determined by energy-dispersive X-ray spectroscopy (EDX) and the morphology by scanning (JEOL-JSM 840) and transmission electron microscopy (JEOL-JEM 100SX). The porous nature of the oxide particles was studied using powder density by pycnometry,¹² within an error of $\sim 5\%$. Surface areas were measured using the BET (Micromeritics Gemini) nitrogen gas adsorption method.

3. Results and Discussion

The crystal structure of Cr_2O_3 is similar to that of corundum ($\alpha\text{-Al}_2\text{O}_3$) and is composed of a regular octahedral CrO_6 group.¹ The Cr_2O_3 structure is an approximately hexagonal close packed array of O atoms in which Cr^{3+} ions occupy two-thirds of the octahedral holes. The symmetry is rhombohedral, but the structure can be visualized more easily using a larger hexagonal unit cell. On the other hand, Mn_2O_3 is known¹ to have two different crystal structures; namely, $\alpha\text{-Mn}_2\text{O}_3$ and $\gamma\text{-Mn}_2\text{O}_3$. $\alpha\text{-Mn}_2\text{O}_3$ belongs to the $\text{C-M}_2\text{O}_3$ structure type (bixbyte structure), which is closely related to that of CaF_2 with tetragonal distortion ($c/a = 1.16$).

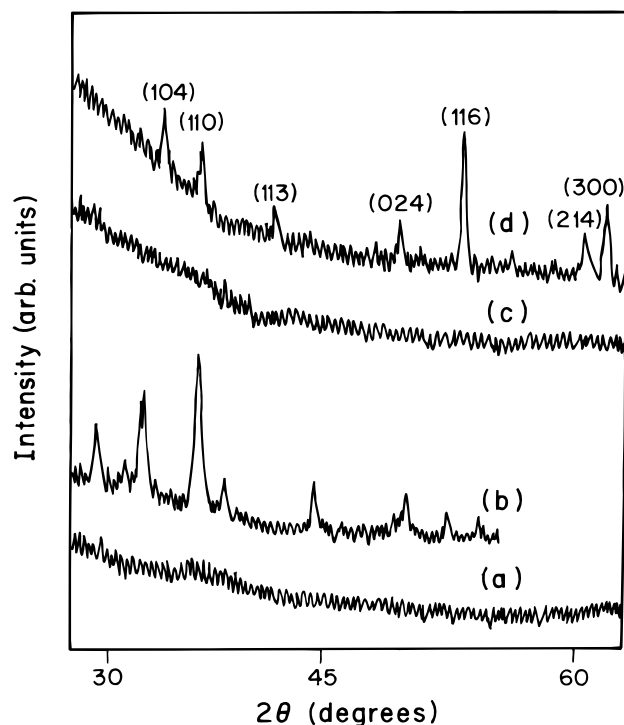


Figure 1. X-ray diffractograms of (a) as-formed Mn_2O_3 , (b) calcined Mn_2O_3 , (c) as-formed Cr_2O_3 , (d) calcined Cr_2O_3 .

Table 1. XRD, DSC, and Elemental Analysis Data of Cr_2O_3 and Mn_2O_3

properties	Cr_2O_3	Mn_2O_3
crystal system	rhombohedral	tetragonal
lattice parameter (Å)	$a = b = 4.9495$ $c = 13.5972$	$a = b = 8.1317$ $c = 9.4413$
crystallization temperature (K)	900 (1125) ^a	600 (775) ^b
elemental analysis ^c		
Cr ^d	70.51(68.47)	
Mn ^d		71.42 (69.61)
K		
N	0.06	
C	1.02	0.43
H	0.34	

^a Values in the parentheses from ref 2d. ^b Values in the parentheses from ref 2e. ^c Amorphous products. ^d Values in parentheses correspond crystalline products.

The X-ray pattern of as-prepared powder [Figures 1a and 1c] shows them to be amorphous. On calcination of the powder obtained from $(\text{NH}_4)_2\text{Cr}_2\text{O}_7$, solutions for 4 h at 900 K and of the powder produced in KMnO_4 at 600 K, the solids show X-ray diffraction pattern characteristics of Cr_2O_3 and Mn_2O_3 with cell dimensions (Table 1) that are in good agreement with literature values (JCPDS card no. 38-1479 for Cr_2O_3 , JCPDS card no. 6-540 for $\alpha\text{-Mn}_2\text{O}_3$). It is interesting to note that, on heating, the sonication-derived Mn_2O_3 forms $\alpha\text{-Mn}_2\text{O}_3$ (bixbyte structure) with a tetragonal distortion (c/a) of ~ 1.16 .

The formation of amorphous Mn_2O_3 and Cr_2O_3 was confirmed by the FT-IR spectroscopy. The FT-IR spectra of KMnO_4 before and after ultrasound irradiation are shown in Figure 2. The strong absorption at ~ 1000 cm^{-1} and a shoulder around 840 cm^{-1} of KMnO_4 before sonication [Figure 2a] correspond to characteristic internal modes of $[\text{MnO}_4]^-$ group (regular T_d symmetry).¹³ The absorption peak at ~ 500 cm^{-1} with a shoulder around 600 cm^{-1} after ultrasound radiation [Figure 2b] corresponds to the vibrational modes of a

(11) *X-ray Diffraction Procedures*; Klug, H., Alexander, L., Eds.; Wiley: New York, 1962; p 125.

(12) *Annual Book of ASTM Standards*, 1989, Vol. 02.05, p B527.

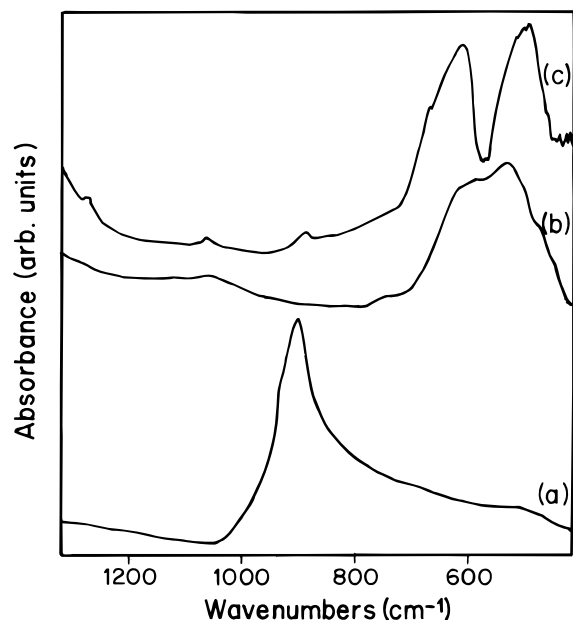


Figure 2. FT-IR spectra of KMnO_4 before (a) and after (b) ultrasound irradiation, (c) calcined insonation oxide residue (Mn_2O_3).

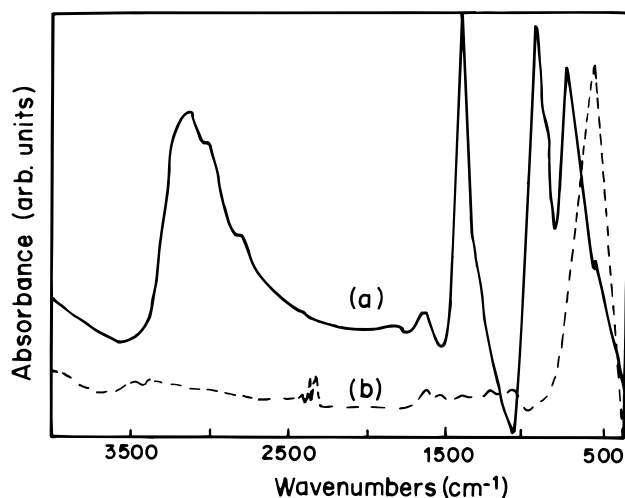


Figure 3. FT-IR spectra of $(\text{NH}_4)_2\text{Cr}_2\text{O}_7$ before (a) and after (b) ultrasound irradiation.

distorted MnO_6 octahedra. The appearance of two distinct absorption peaks around 500 and 600 cm^{-1} for the calcined sample [Figure 2c] implies a distorted octahedral symmetry of $\alpha\text{-Mn}_2\text{O}_3$.

The FT-IR spectrum of $(\text{NH}_4)_2\text{Cr}_2\text{O}_7$ before sonication [Figure 3a] shows four strong absorption peaks in the frequency region of 500–4000 cm^{-1} . The absorption peaks at ~ 3150 and 1400 cm^{-1} are ascribed to the N–H vibrational modes of $[\text{NH}_4]^+$ groups,¹³ while two sharp absorptions at ~ 950 and 750 cm^{-1} correspond to characteristic internal modes of the $[\text{Cr}_2\text{O}_7]^{2-}$ group. The FT-IR spectrum of the insonation product of $(\text{NH}_4)_2\text{Cr}_2\text{O}_7$ [Figure 3b] replaces these four absorption peaks by a single strong one at ~ 580 cm^{-1} , corresponding to the characteristic vibrational mode of symmetric CrO_6 octahedra of Cr_2O_3 . A small hump between 3700 and 3300 cm^{-1} corresponds to the ν_{OH} of water.

(13) *Infrared Spectra of Inorganic and Coordination Compounds*; Nakamoto, K., Eds.; Wiley: New York, 1963; pp 107–119.

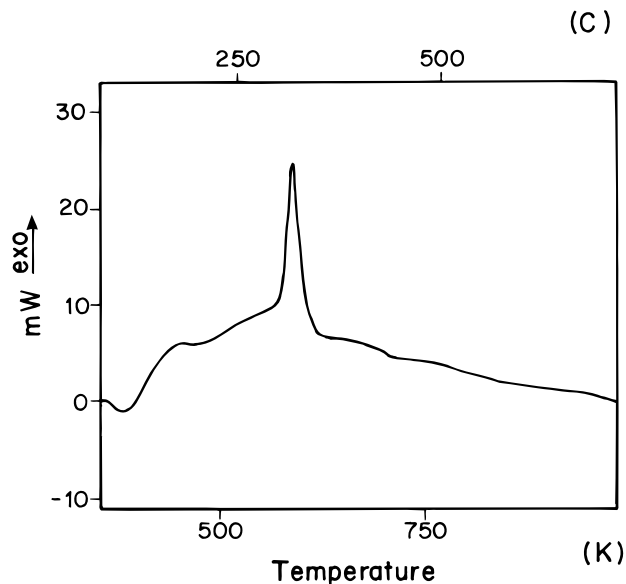


Figure 4. DSC profile of insonation oxide residue of KMnO_4 .

The DSC profile of Mn_2O_3 (Figure 4) shows a sharp exothermic peak around 600 K, which is attributed to the crystallization of amorphous Mn_2O_3 . The small endothermic peak at ~ 100 °C is probably due to the elimination of trapped solvents. On the other hand, Cr_2O_3 displays its crystallization peak at 900 K (exotherm). The observed crystallization temperatures are much lower than that of the powders, obtained by traditional preparation methods (see Table 1). This lower crystallization temperature of sonication-derived oxide powders could be attributed to their ultrafine nature.

The results of elemental analysis along with the XRD, DSC data are summarized in Table 1. The presence of small amounts of impurities (C and H) is presumably caused by decomposition products of the cosolvent (ethanol). Both the elemental analysis and the EDX results of both amorphous oxides showed a higher percentage of metal content than the expected theoretical value, while the crystalline products obtained by calcination are stoichiometric Cr_2O_3 and Mn_2O_3 .

The higher concentration of the metal ion in the amorphous oxide may be due to the presence of $\text{M}_2\text{O}_{3-\delta}$ defects, which may be due to the rapid quenching attained during cavitation and ultrasound-driven collision between the solid particles in the sonochemical process.⁴ The defect-structured amorphous oxide materials are of prime importance in electronic and catalytic applications due to their unique properties.¹⁴ Apart from the ultrafine nature, the presence of defect sites seems to be responsible for the low temperature of crystallization of these powders.

The particulate properties of the amorphous oxide powders are summarized in Table 2. The powder density is 45–50% of the theoretical value indicating the porous nature of the insonation oxide powders. The surface area of Cr_2O_3 is 35 m^2/g and that of Mn_2O_3 is 48 m^2/g . The TEM micrographs of Cr_2O_3 powder [Figure 5a] shows that the particles are nearly spherical in shape with smooth surface and highly agglomerated nature. The actual size of the particle measured from

(14) Carnell, P. J. H.; Starkey, P. E. *Chem. Eng.* **1984**, 408, 30.

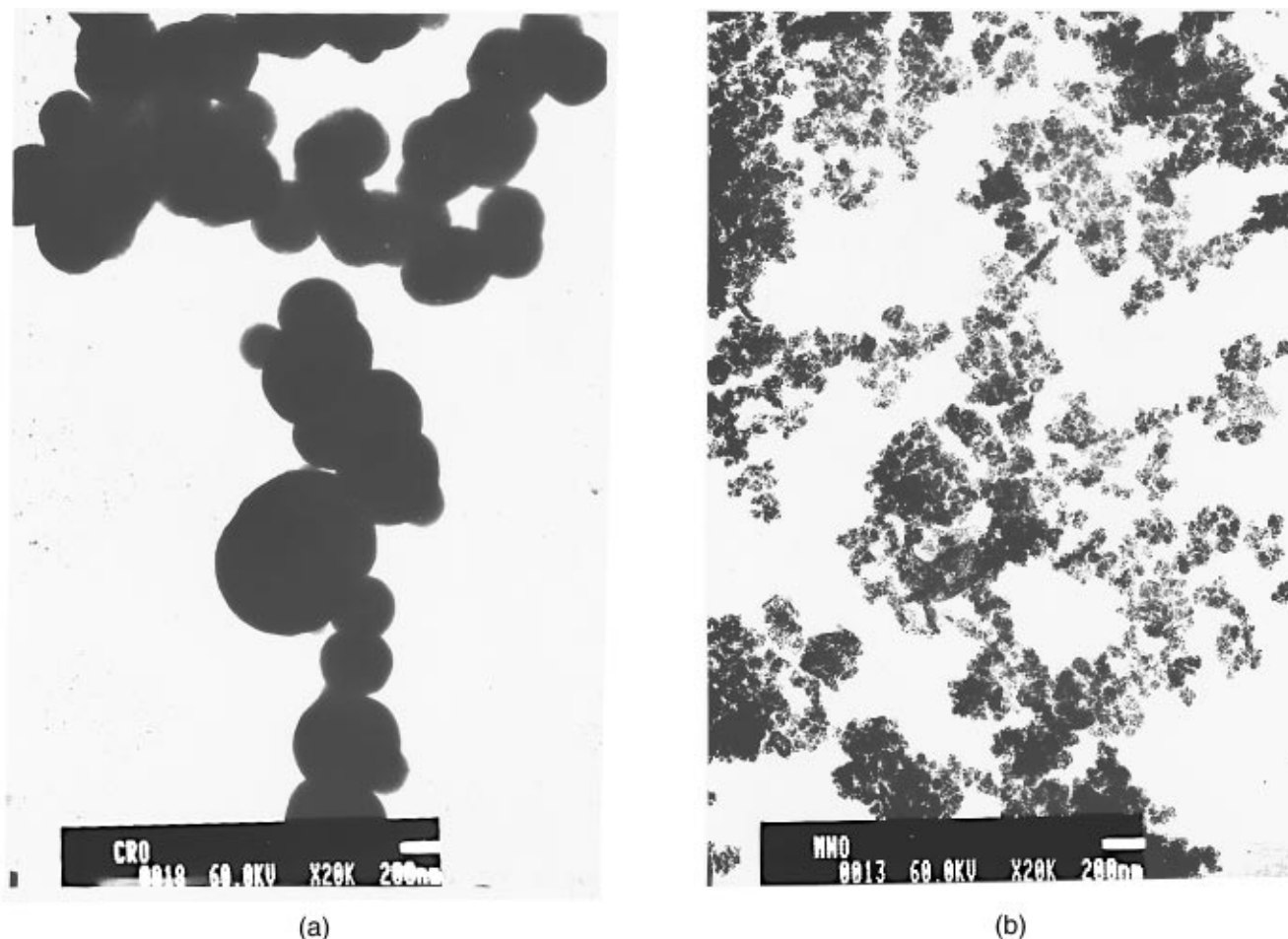


Figure 5. Transmission electron micrograph of amorphous (a) Cr_2O_3 and (b) Mn_2O_3 .

Table 2. Particulate Properties of Amorphous Cr_2O_3 and Mn_2O_3

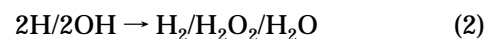
properties	Cr_2O_3	Mn_2O_3
powder density (g/cc)	2.66	2.34
surface area BET (m^2/g)	35	48
calculated particle size ^a (nm)	64	53
actual particle size ^b (nm)	200	50
particle morphology ^b	spherical	irregular
nature of agglomeration ^b	hard	soft

^a From surface area and density. ^b From TEM.

TEM pictures is 200 nm, which is much higher than the calculated value (using surface area and density). This discrepancy in the calculated particle size is due to the assumption that the particles are nonporous and its complete neglect of the extent of agglomeration. On the other hand, the Mn_2O_3 particles are irregularly shaped with a rough surface and fluffy nature [Figure 5b]. The particles are nanosized with an average size of 50 nm, which coincides with that the calculated value. The domain size of the crystalline Cr_2O_3 and Mn_2O_3 was 340 and 85 nm, respectively, as calculated from the XRD line broadening. The increase in the size of the particles after calcination presumably is due to the sintering of ultrafine particles upon crystallization.

It has been reported that three different regions are formed in the aqueous sonochemical process:^{7,15-18} (1) The inside of the collapsing bubble where elevated

temperatures (several thousands of degrees) and high pressures (hundreds of atmospheres) are produced, causing water vapor to pyrolyze into H atoms and OH radicals. (2) The interfacial region between the cavitation bubbles and the bulk solution where the temperature is lower than that inside cavitation bubble, but still high enough for thermal decomposition of solutes to occur. (3) The bulk solution at ambient temperatures where reactions takes place between solute molecules with OH radicals or H atoms, which escaped from the interfacial region. Of the aforementioned three regions, we prefer the interfacial zone as the region where the major part of the reduction takes place, since the low vapor pressure of the reactants would require that only a minor part of the reduction would happen inside the cavity. The mechanism involved in the reduction process must take into consideration with regard to the species generated from the water molecules by the absorption of ultrasound. The likely explanation for the sonochemical reduction process is summarized below:



In the absence of any additives or scavengers, the H and OH radicals readily recombine to give the products

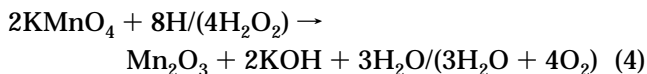
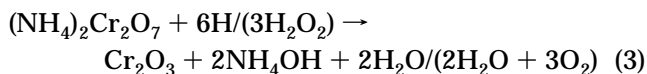
(15) Gutierrez, M.; Henglein, A. *J. Phys. Chem.* **1988**, *92*, 2978.

(16) Okitsu, K.; Bandow, H.; Maeda, Y.; Nagata, Y. *Chem. Mater.* **1996**, *8*, 315.

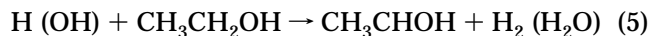
(17) Asmus, K.-D.; Mockel, H.; Henglein, A. *J. Phys. Chem.* **1973**, *77*, 1218.

(18) Mulvaney, P.; Dension, L.; Grieser, F.; Cooper, R.; Sanders, J. V.; Meisel, D. *J. Colloid Interface Sci.* **1988**, *121*, 70.

shown in eq 2.⁷ The formed H₂O₂ (eq 2) can also act as a reducing species in the presence of the strongly oxidizing [MnO₄]⁻ and [Cr₂O₇]²⁻ species.¹⁹ Therefore, the sonochemical reduction of reactants to the corresponding oxides by the reducing radicals are consistent with the following reactions [eqs 3 and 4].

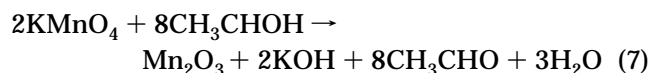
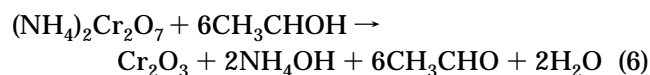


The acceleration of the sonochemical reduction process by the addition of ethanol is attributed to the formation of secondary reducing radicals by the combination of CH₃, CH₃CHOH (α -hydroxyethyl radical), and others formed by the pyrolysis of ethanol by ultrasound irradiation.^{7,15} These radicals can react with themselves or with H or OH radicals to yield various reducing radicals, which in turn help to accelerate the reduction process. According to Grieser et al.^{7,9,18} the attack of the ethanol by H atoms or OH radicals yields an α -hydroxyethyl radical:



It has been well documented that α -hydroxyalkyl radicals are more likely to initiate the reduction process.^{17,18} Therefore, the sonochemical reduction of the corre-

sponding reactants in the presence of ethanol in an aqueous medium can be written as follows.



On the basis of the general observation in sonochemistry that raising the solution temperature lowers the chemical yield,⁴ the observed increase in yield of oxide with an increase in bulk solution temperature cannot be attributed to the sonochemical effect; it could be due to an enhanced thermal reaction.

In conclusion, ultrafine amorphous oxide powders of Cr₂O₃ and Mn₂O₃ have been successfully generated by an aqueous sonochemical reduction method at around room temperature. The major advantage of the sonochemical method, apart from its fast quenching rate and operation at ambient conditions, is that it is a simple and energy-saving process. This method raises the possibility of the preparation of technologically important simple and mixed transition metal oxides.

Acknowledgment. A. Gedanken thanks the Ministry of Science and Technology for supporting this research through the Israel-India grants program. Y. Kolytyn thanks The Ministry of Absorption, The Center for Absorption in Science, for its financial help. The authors thank Professor M. Deutsch, Department of Physics, for extending the XRD facility to us.

CM9704645

(19) *Advanced Inorganic Chemistry*; Cotton, F. A., Wilkinson, G., Eds.; Interscience, Wiley: New York, 1964; pp 280-282.